Details of Da Vinci Aerial Screw Physics, Aerodynamics and Performance

Koushik Marepally† Postdoctoral Research Associate
Ron Berlin† Undergraduate Student
James Baeder† Professor

†Alfred Gessow Rotorcraft Center, University of Maryland, College Park, MD, USA

ABSTRACT

This study investigates the aerodynamic complexities of aerial screws, inspired by Leonardo da Vinci's visionary 16th-century designs. Through Computational Fluid Dynamics (CFD) analysis, the investigation unveils a vortex-based thrust mechanism analogous to vortex lift observed in swept and delta wings. The key 'da Vinci' vortex, a shape-conforming helical structure at the screw's tip, serves as a focal point for evaluating the influence of design variables on aerodynamic efficiency. Detailed analyses of screw pitch and taper reveal nuanced effects on thrust generation, offering valuable insights for optimizing aerial screw performance. This work provides a comprehensive understanding of historical roots and contemporary advancements in aerial screw technology, paving the way for efficient Vertical Take-Off and Landing (VTOL) alternatives.

INTRODUCTION

The concept of aerial screws, designed for vertical flight, traces its roots back to the ingenious mind of Leonardo da Vinci in the 1500s, as depicted in Figure 1. Later efforts to realize this visionary concept resulted in the construction of a high-solidity helicopter in the late 1800s (Ref. 1). Several early experimental attempts to understand the physics of screw type propellers were inconclusive (Ref. 2) due to the difficulties in fabricating these structures and the low precision and accuracy in experimentally measured data. Despite these early efforts, the aerial screw was eventually overshadowed by conventional rotors with large aspect ratios, low solidity, and airfoil blades, which proved more effective for vertical flight. With advancements in heavier-than-air-flight sciences, these designs were subsequently left unstudied.

Much later, these designs were revisited in the context of the VFS annual design competition in 2020 (Ref. 3). A series of contemporary vehicle designs (Ref. 4), inspired by the classical aerial screw, were meticulously developed and studied for a simple hovering mission profile. This exploration marks a significant leap forward, utilizing modern analysis tools to delve into and comprehend the intricate physics underpinning aerial screws. The culmination of this effort is showcased through the development of a working prototype for a small-scale UAV employing aerial screws (Refs. 5, 6), offering a compelling proof-of-concept for the thrust generation capabilities inherent in this innovative design. Preliminary designs, estimating figures of merit up to 0.52 (Ref. 4), highlight the significant potential of these rotors in VTOL and hovering applications.

Figure 1. Leonardo's Aerial Screw depicted in the page of Paris Manuscript B, folio 83v

Central to the thrust generation mechanism of aerial screws is the ”da Vinci” vortex (Ref. 4), a shape-conforming helical vortical structure at the screw's tip. The strength of this vortex determines the pressure distribution on the screw's surface and, consequently, the rotor's efficiency. Leveraging the use of modern modeling and simulation tools, the current study aims to unravel the effects of different design variables on the

”da Vinci” vortex and the overall efficiency of the aerial screw.

“DA VINCI CODE”: THE THRUSTING MECHANISM OF AERIAL SCREW

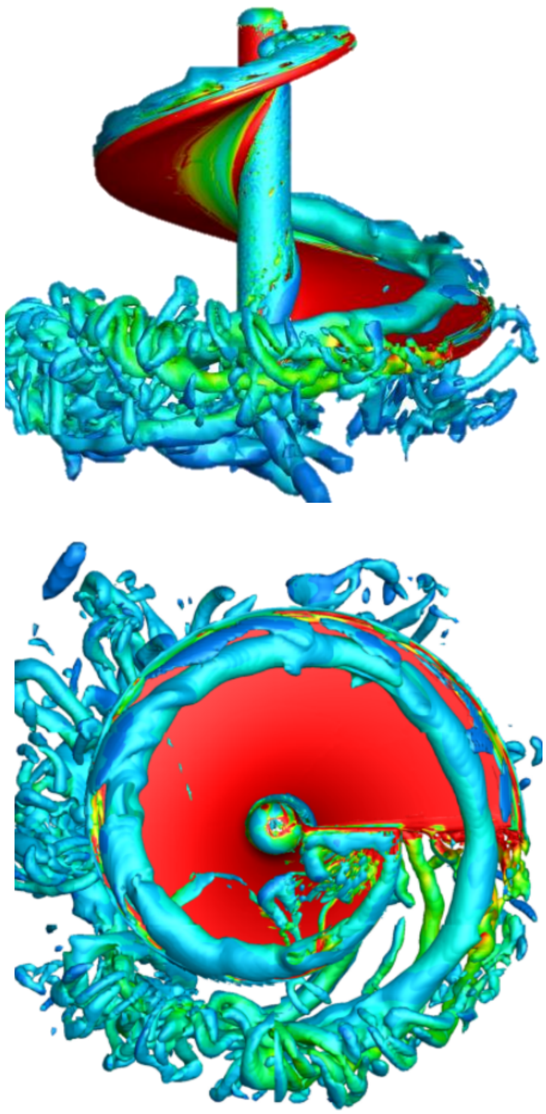

Figure 2. Iso-surfaces of vorticity Q-criterion around a notional hovering aerial screw (top: side view, bottom: top view)

A detailed understanding of the thrusting mechanism within aerial screws is achieved through Computational Fluid Dynamics (CFD)-driven discovery of the flow physics. The thrusting mechanism bears analogies to vortex lift (Ref. 7), an aerodynamic phenomenon of non-linear lift, observed in highly swept and delta wings. Illustrated in Figure 2, the vorticity iso-surface in the flow field show a shape-conforming helical vortical structure on the top surface of a hovering aerial screw. This vortex induces suction, generating a substantial pressure disparity across the screw surface and consequently contributing to an effective thrust component.

The initiation of the vortical structure’s development occurs due to a circulation along the leading edge, where the screw edge meets the freestream. Subsequently, the span-wise vortex moves downstream and rolls up along the screw surface, resulting in the formation of a tip vortex. Further, the presence of taper on the screw surface creates a delta wing-like aerodynamic environment, continuously adding to the strength of the vortex along the blade tip, resulting in a shape conforming helical vortical structure viz. the “da Vinci” vortex. This increases the proportion of the screw surface active in thrust generation. However, it must be noted that the inboard sections of the screw surface exhibit a comparatively insignificant contribution to the overall thrust generation.

GEOMETRIC DEFINITION OF AERIAL SCREW: DESIGN VARIABLES

The geometry of a typical screw, including an aerial screw, is primarily defined by its radius, pitch, and the number of turns. Pitch of the screw is the length the screw surface advances in the axial direction for one full rotation of the screw. Radius of the screw is the radius of the screw surface projected perpendicular to the axial direction and the number of turns is the total number of full rotations of the screw surface in the azimuthal direction of the screw. For simplicity and due to the impracticality of long, towering screws, the number of turns of the screw is chosen to be 1 throughout this study.

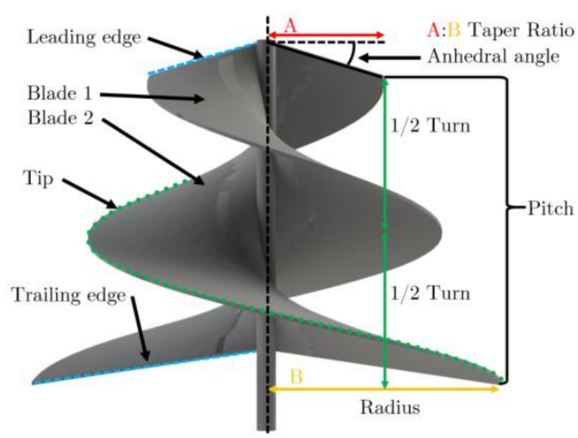

Figure 3. Design variables defining the geometry of a screw

Modern variations of the screw designs include addition of a taper to the screw as well as a dihedral angle between the screw surface and the axial plane. The taper ratio is defined as the ratio between the local screw radii across one full turn of the screw surface. Figure 3 shows different design variables that define the aerial screw geometry. This study excludes the investigation of dihedral angle effects on screw aerodynamics.

Mathematically, the aerial screw designs are defined using the non-dimensional variables and appropriate scaling parameters corresponding to each of these design variables.

Radius of the Screw

The radius of the screw is defined on a projection perpendicular to the screw's axial direction. Since the local radius of the screw can vary due to taper, the radius of the screw is defined as the radius of the projection corresponding to the maximum radius location ($R_{\max}$), i.e., trailing edge. This radius is used as the length scale for non-dimensionalization of other variables and physical quantities. The disc area corresponding to this radius is used as the reference surface area for load coefficients.

A local non-dimensionalization of the radial coordinate is also applied using R_{local}, which is the maximum radius at a particular azimuthal section.

$$r' = \frac{r}{R_{\text{local}}} \tag{1}$$

Pitch Rate

The screw pitch rate is defined as the axial length that the screw advance for one full rotation of the screw. For a linearly pitching screw, the advancement per unit change in the screw rotational coordinate is constant throughout the screw surface, i.e., the pitch rate is constant. However, the designs can also have a non-uniform pitch rate, i.e., the screw advances at different rates as the screw rotates at different azimuthal orientations. Within the scope of this study, two different variations of pitch rates are studied, viz., uniform (linear pitch) and bilinear pitch. The bilinearly pitched screw has a different uniform pitch rate for the first and second halves of the screw.

This quantity is non-dimensionalized using the maximum radius of the screw. Thus, if the screw has a pitch rate of ζ, then the screw advances $R_{\max}\zeta\Delta N$ when the screw turns by ΔN rotations. It must be noted that the bilinear taper rate is also non-dimensionalized using the same maximum radius of the screw.

$$\zeta = \frac{1}{R_{\max}}\frac{\Delta Z}{\Delta N} = \frac{2\pi}{R_{\max}}\frac{\Delta Z}{\Delta \theta} \tag{2}$$

Due to a uniform pitch rate, the inboard and outboard section advance the same axial distance per unit change in azimuthal coordinate. Thus, the screw surface has a steeper gradient in the inboard sections compared to the outboard sections, which affect the contributions of the blade normal forces to the axial thrust component. Similarly, as the pitch rate increases, the surface gradient also becomes steeper, resulting in a decreased contribution of normal force to axial loads and an increased contribution to the torque-wise component.

Figure 4 shows the axial component of the surface normal unit vector of aerial screws with different pitch rates, indicating the loss in contribution to thrust for higher pitch rate ($\zeta = 1.3$) compared to lower pitch rate ($\zeta = 1$). The figures show screw projections onto $r' - \theta$ plane, i.e., the radial coordinate is the locally non-dimensionalized radius and the azimuthal coordinate corresponds to clockwise orientation (since the screw rotates in anti-clockwise direction). The azimuth zero corresponds to the leading edge of the screw blade and then becomes the trailing edge after one full clockwise rotation.

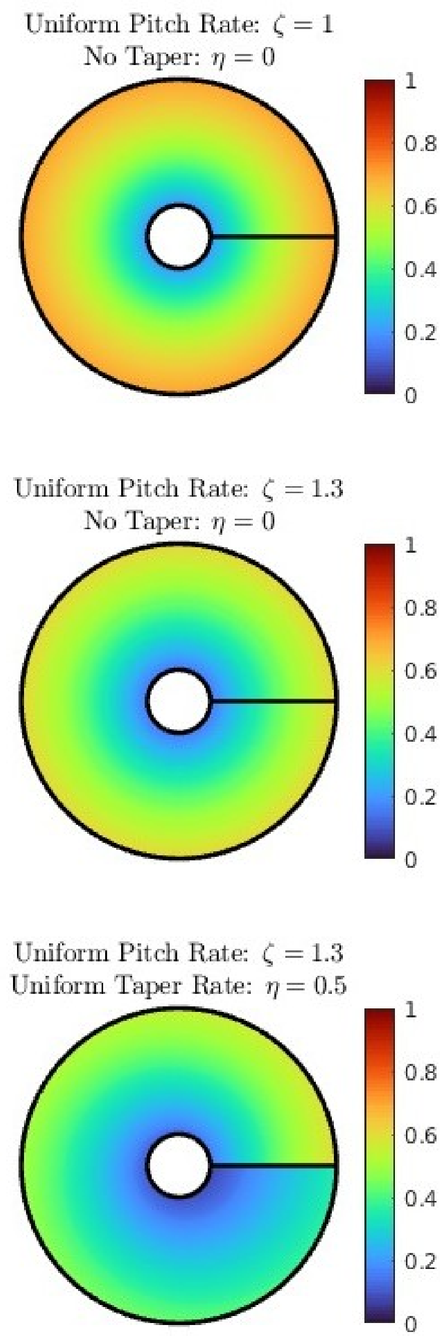

Figure 4. Axial component of the local surface unit normal vector for screws with different pitch and taper rates showing the contributions of pressure to the thrust of aerial screw

Taper Rate

The screw taper rate is defined as the reduction of the local tip radius (R_{local}) of the screw for one screw rotation. For a linearly tapered screw, the reduction in local tip radius per unit change in the screw rotational coordinate is constant throughout the screw surface, i.e., the taper rate is constant. However, the designs can also have a non-uniform taper rate, i.e., the screw tapers at different rates as the screw rotates at different azimuthal orientations. Within the scope of this study, two different variations of taper rates are studied, viz., uniform (linear taper) and bilinear taper. The bilinearly tapered screw has a different uniform taper rate for the first and second halves of the screw.

This quantity is non-dimensionalized using the maximum radius of the screw. Thus, if the screw has a taper rate of η, then the local tip radius increases by $\eta R_{\max}\Delta N$ when the screw turns by ΔN rotations. It must be noted that the bilinear taper rate is also non-dimensionalized using the same maximum radius of the screw.

$$\eta = \frac{1}{R_{\max}}\frac{\Delta R_{\text{local}}}{\Delta N} = \frac{2\pi}{R_{\max}}\frac{\Delta R_{\text{local}}}{\Delta \theta} \tag{3}$$

Due to a uniform taper rate, the azimuthal sections closer to the leading edge have a smaller local radius compared to the sections towards the trailing edge. To maintain a same pitch rate, the screw surface has a steeper gradient in the upstream sections compared to the downstream sections of the blade, which affect the contributions of the blade normal forces to the axial thrust component.

Figure 4 compares the axial component of the surface normal unit vector for screws with and without taper at a constant pitch rate, indicating a lower contribution of the upstream sections compared to downstream sections.

Number of Blades

The number of blades is a crucial factor for rotor balancing and vibration control. A single bladed screw experiences minimal aerodynamic interactional effects compared to multiple blades. However, due to the pitch and taper of the screw, the rotor center of mass moves away from the axis of rotation and induces vibrations and large inertial loads on the hub. Two bladed rotors overcome this problem by balancing the rotor blade mass with a counter mass through the second blade. Further increase in blades reduces the moments of interia about in-plane axes. In this study, a comparison of aerodynamics for one, two and three bladed rotors is investigated.

INFLUENCE OF DESIGN VARIABLES ON AERIAL SCREW AERODYNAMICS AND PERFORMANCE

The main aim of this study is to identify the influence of each of the design variables that define the aerial screw geometry on the performance, and understand the variations in flow physics attributing to the changes in performance. The performance comparison is performed for a constant thrust requirement for different screws, with figure of merit as a metric of the performance.

Computational Fluid Dynamics (CFD) is used for the aerodynamic analysis of the flow around these hovering screws using HAMSTR (Ref. 8), UMD's in-house CFD solution framework. HAMSTR employs Hamiltonian paths and strand grids based solution methodology, coupled with overset meshes for farfield computations. DDES (Delayed Detached Eddy Simulation) is the mathematical model used to describe the flow, with SA (Spalart-Allmaras) turbulence closure model, and fully turbulent flow assumptions.

The da Vinci vortex strength and the local screw aerodynamics are compared by means of the pressure difference across top and bottom surface of the screw, to explain the influence of the design variables on the aerodynamics. These comparisons are presented as contours on the projected screw surface in $r' - \theta$ plane.

Effect of Radius ($R_{\max}$)

To investigate the effect of screw size ($R_{\max}$) on the performance, five different screws are modeled with a uniform pitch rate ($\zeta = 1$) and uniform taper rate ($\eta = 0.5$), viz., $R_{\max} \in \{0.25 \text{ ft}, 0.5 \text{ ft}, 1 \text{ ft}, 5 \text{ ft}, 10 \text{ ft}\}$. The RPM of the screws is chosen to attain a tip Mach number of 0.25 at the tip of the trailing edge of the blade. Due to the variation in size, the tip Reynolds number varies from 0.5×10^6 to 17×10^6.

Figure 5 shows the variation of figure of merit across for different screw sizes. It is observed that as the screw size increases, the figure of merit of the screw increases with a larger variation at lower sizes and smaller variations at larger sizes. The da Vinci vortex development is similar across all the sizes and shows similar pressure differences ΔC_P across the blade surface.

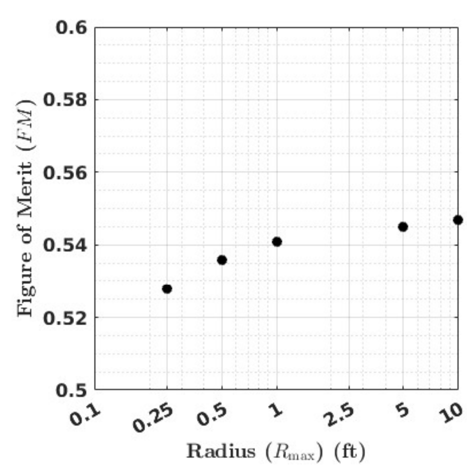

Figure 5. Variation of Figure of Merit for Screws of different sizes

Minor variations in the figure of merit can be attributed to the viscous effects contributing to higher power requirements and resulting in lower efficiency as the radius decreases (and the Reynolds number decreases).

Effect of Pitch Rate (ζ)

To understand the effect of pitch rate, several screws with a constant taper rate $\eta = 0.5$ and $R_{\max} = 1$ ft are studied, with each screw having a different uniform pitch rate. The tip Mach number at the trailing edge is maintained at 0.25 for all these screw designs, which corresponds to a tip Reynolds number of 1.7×10^6.

Figure 6 shows the variation of figure of merit for these screws with the pitch rate. It can be seen that the performance of the screw improves initially when the pitch rate ζ increases from 1 to 1.2, and then decreases continuously with increasing pitch.

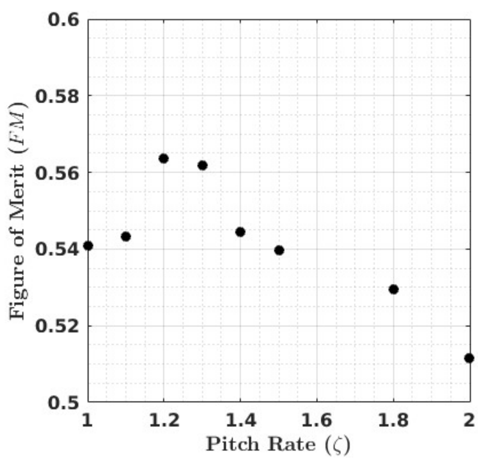

Figure 6. Variation of figure of merit of aerial screws with varying pitch rate

The aerodynamic behavior of the high pitched screw results in a large shed vorticity at the leading edge due to flow separation, resulting in a stronger tip vortex formation. Figure 7 shows the pressure difference across the blade surface for three different screws with low ($\zeta = 1$), moderate ($\zeta = 1.2$) and aggressive ($\zeta = 1.5$) pitch rates. It can be seen that the leading edge shed vorticity and the corresponding pressure difference can be seen as continuously increasing with increasing pitch rate.

However, the normal force (ΔC_P) due to the vortex contributes to both thrust and torque. Figures 8, 9 show the axial and torque-wise components of the pressure loads projected onto $r' - \theta$ plane. As the pitch rate increases from 1 to 1.2, the axial contribution of the normal force increases significantly. This is due to a significant increase in ΔC_P accompanied by a moderate decrease in axial component, resulting in effectively larger increase in the resultant axial loads. As the pitch rate is further increased aggressively to 1.5, the axial projection component decreases significantly compared to the increase in ΔC_P. As a resultant, the axial contribution of the normal force increases slightly.

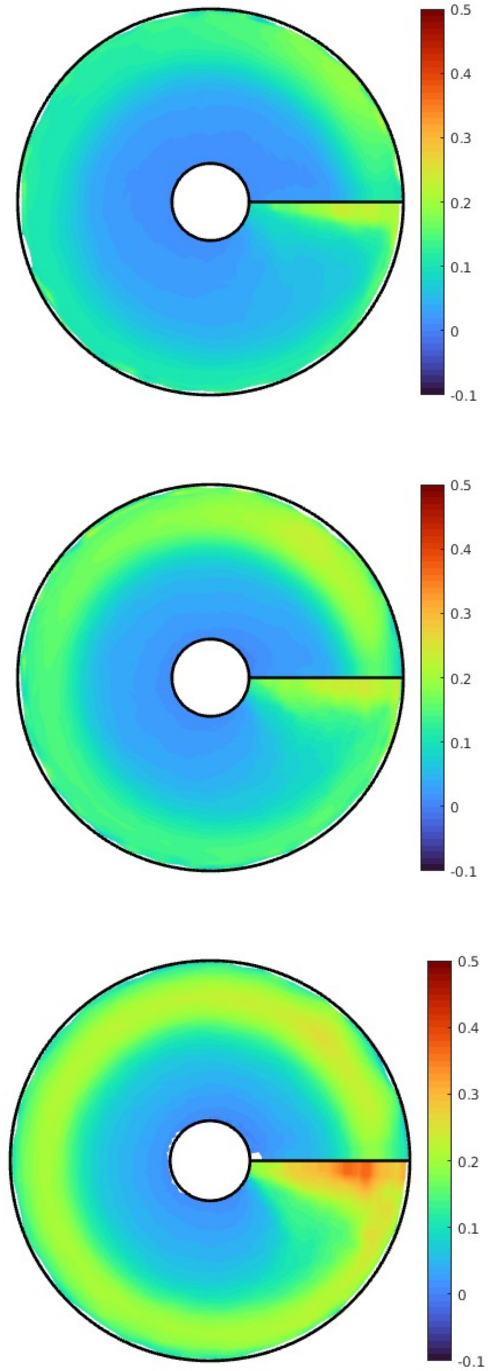

Figure 7. ΔC_P contours for aerial screws with different pitch rates: Top: $\zeta = 1$, Middle $\zeta = 1.2$ and Bottom: $\zeta = 1.5$

The change in axial loads corresponding to the variation from low to moderate pitch rate is observed to be $\sim 36\%$, while that corresponding to moderate to aggressive pitch rate is $\sim 15\%$. The ideal power change corresponding to this increase in axial load is given by the percentage change of $C_T^{3/2}$. This amounts for approximately 58% for the low to moderate pitch rate and 23% for the moderate to aggressive pitch rate variation.

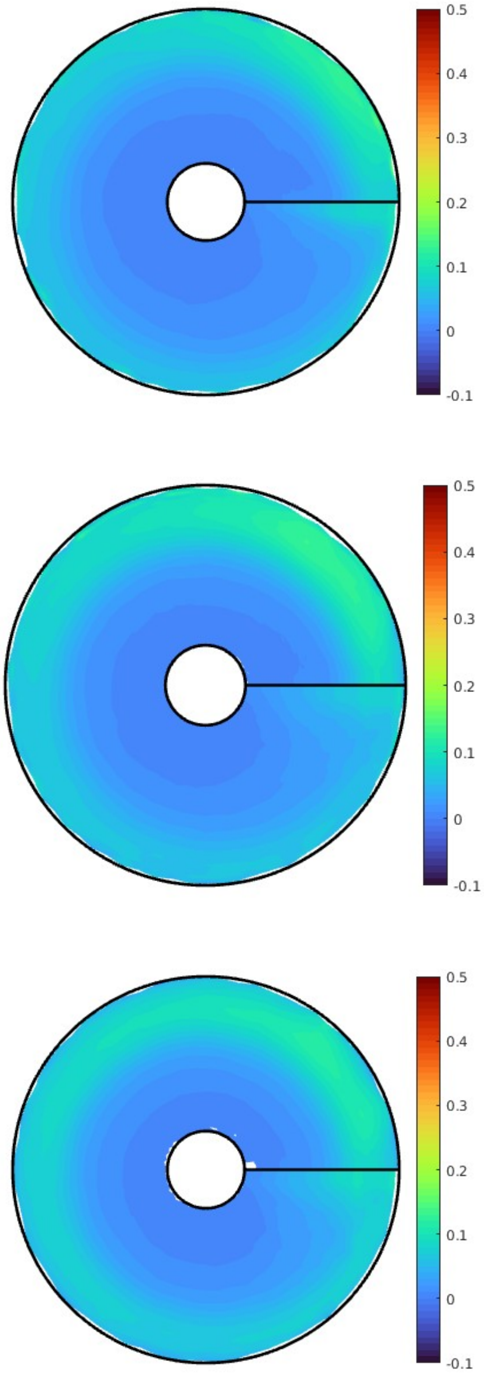

Figure 8. Axial component of ΔC_P contours for aerial screws with different pitch rates: Top: $\zeta = 1$, Middle $\zeta = 1.2$ and Bottom: $\zeta = 1.5$

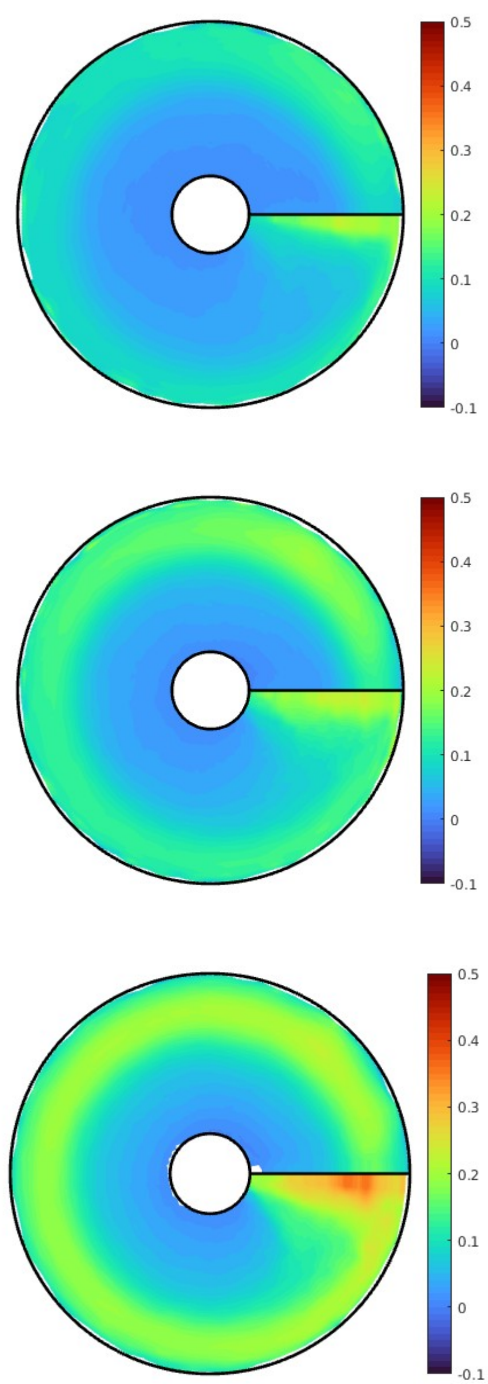

Figure 9. Torque-wise component of ΔC_P contours for aerial screws with different pitch rates: Top: $\zeta = 1$, Middle $\zeta = 1.2$ and Bottom: $\zeta = 1.5$

When the torque-wise components for these scenarios are compared, the torque contribution increases moderately from low to moderate pitch variation, but increases significantly for the high pitch screw. The torque-wise load, i.e., actual power variation is observed to be $\sim 52\%$ for the low to moderate pitch variation. This is less than the ideal power variation computed, indicating that the increase in pitch rate to moderate values has better power characteristics than low pitch rate screw. On the other hand, the power is observed to increase by $\sim 30\%$ for the moderate to aggressive pitch variation, which is higher than the ideal power variation, indicating a poor performance characteristic of the aggressively pitched screw.

Understanding the variation of the surface aerodynamics indicate the effects of aggressive pitch to be detrimental to the

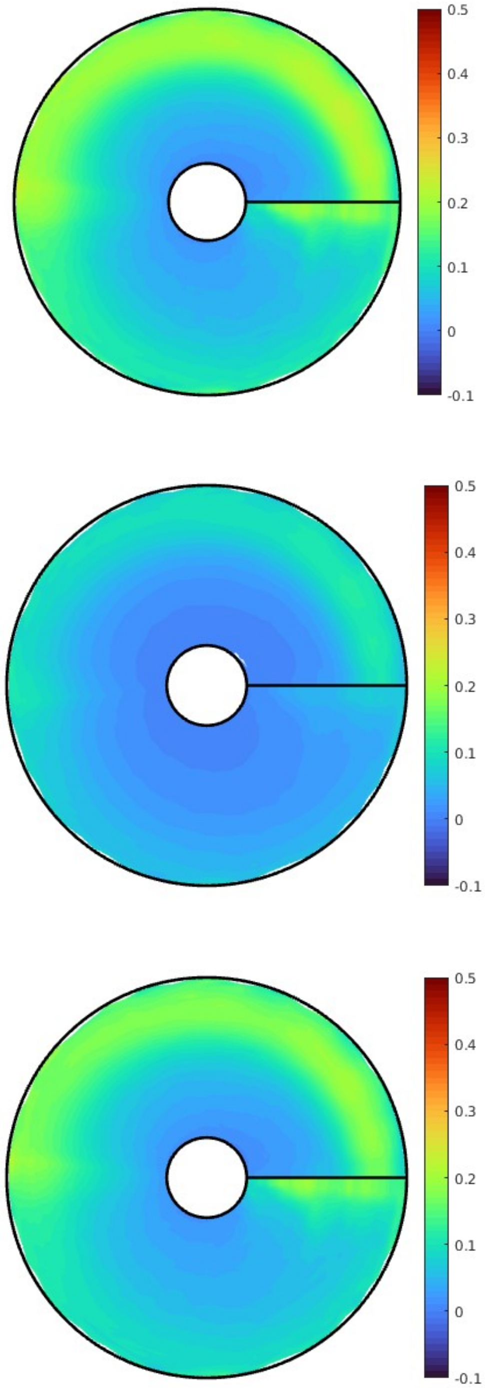

Figure 10. Surface load projections onto $r' - \theta$ plane for the bilenear pitch screw with $\zeta = 1$ for upstream half and $\zeta = 1.4$ for downstream half, Top: ΔC_P, Middle: Axial component and Bottom: Torque-wise component

performance of the screw. A uniform pitch rate essentially causes a larger slope at the tip for a tapered screw near the leading edge as compared to the trailing edge. This indicates a possibility of improvement through non-linear variation of pitch to low-moderate rates closer to the leading edge and increased pitch rates towards the trailing edge. This effect is investigated using a simple bilinear pitch distribution, given by uniform pitch rate for the first and second halves of the screw. The best performing uniform pitch case of $\zeta = 1.2$ is chosen as the baseline. To achieve the same pitch for one full revolution, the pitch rates of bilinear case are decreased and increased in the upstream and downstream halves respectively by the same amount $\Delta\zeta = 0.2$.

Figure 10 shows the normal force and the axial and torque-wise components for the bilinearly pitched screw. It can be observed that this variation of pitch results in a weaker da Vinci vortex in the first half of the screw followed by a stronger vortical structure in the second half. The axial contribution of the corresponding surface loads is similar to the aggressive pitch scenario in the second half and low pitch scenario in the first half. However, even with the aggressive taper in the second half, the torque-wise component shows similarities to moderate pitch scenario in the second half and low pitch scenario in the first half. This improved the overall axial loads by $\sim 3\%$ corresponding to an ideal power increment of $\sim 6\%$. However, the actual power requirements increased by $\sim 5\%$, resulting in a slight increase in the figure of merit by 0.5%.

Effect of Taper Rate (η)

Similar to the effect of pitch rate, the effect of taper rate on the performance of the screw is studied by comparing the screws with all other design variables unaltered. Several screws with a constant pitch rate $\zeta = 1.3$ and $R_{\max} = 1$ ft are studied, with each screw having a different uniform taper rate. The tip Mach number and the tip Reynolds number are maintained the same.

Figure 11 shows the variation of figure of merit for these screws with the taper rate. It can be seen that the performance of the screw continuously decreases as the taper rate is increased beyond 0.5.

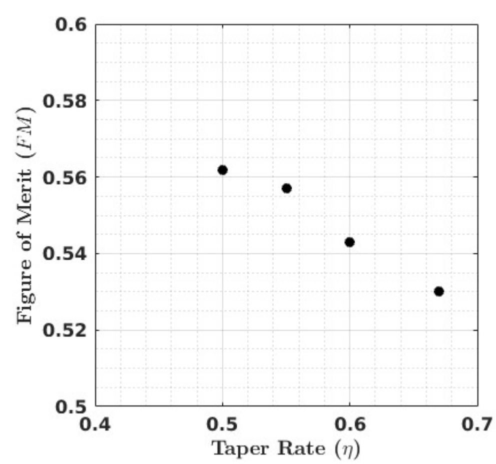

Figure 11. Variation of figure of merit of aerial screws with varying taper rate

Figure 12 shows the projected surface loads and components for the aerial screw with a taper rate of $\eta = 0.5$. Figure 13

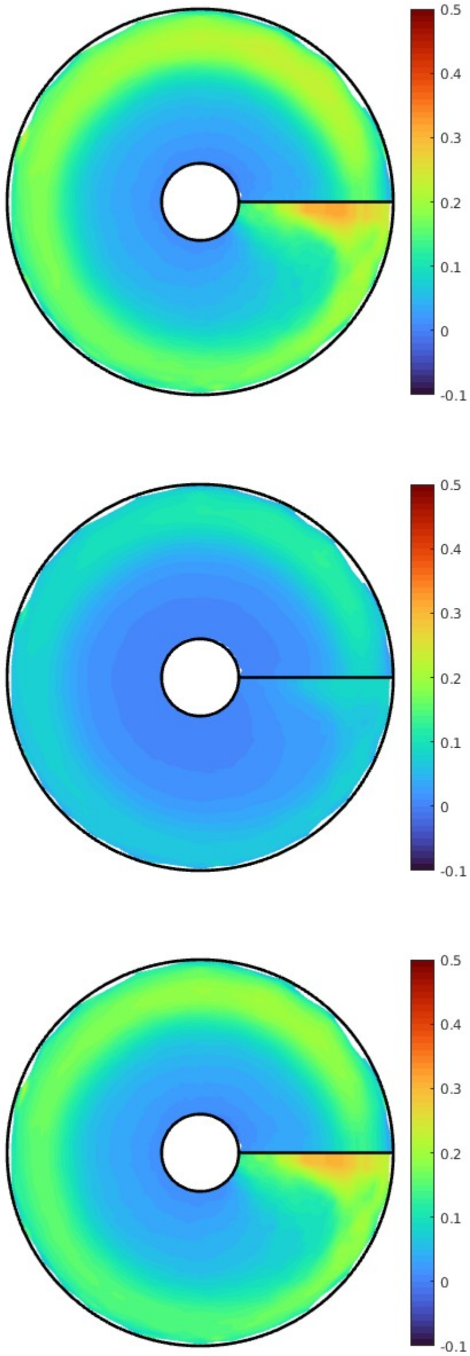

Figure 12. Surface load projections onto $r' - \theta$ plane for aerial screw with $\zeta = 1.3$ and $\eta = 0.5$, Top: ΔC_P, Middle: Axial component and Bottom: Torque-wise component

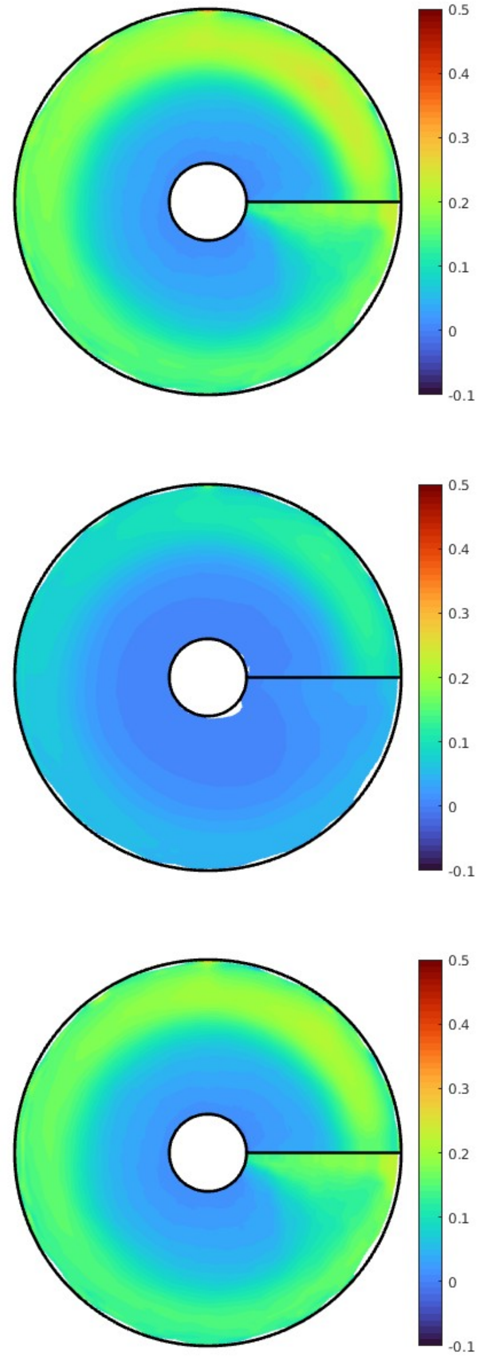

Figure 13. Surface load projections onto $r' - \theta$ plane for aerial screw with $\zeta = 1.3$ and $\eta = 0.67$, Top: ΔC_P, Middle: Axial component and Bottom: Torque-wise component

shows similar projections for the aggressively tapered aerial screw with $\eta = 0.67$. It can be seen that the strength of the da Vinci vortex is similar for both the taper rates, with variations observed at the leading edge. The aggressively tapered screw shows minimal separation due to the extremely small aspect ratio and subsequent tip relief effects at the leading edge. However, the vortex strength is continuously fed in due to a more aggressive taper rate, resulting in a similar downstream characteristics of the da Vinci vortex. The effective lifting area of the screw is reduced with increasing taper, resulting in reduction in both axial and torque-wise loads.

The reduction in axial loads from moderate to aggressive taper are observed to be $\sim 8.5\%$, which corresponds to an ideal power reduction of $\sim 13\%$. However, the actual power requirement is reduced by $\sim 7.5\%$, indicating poor performance of the aggressively tapered screw. The additional power requirements can be attributed to the effects of radial flow which are more prominent in the aggressively tapered screw.

To understand the effect of nonlinear taper, a bilinear variation of taper is developed where the first half of the screw has a uniform taper rate and the second half is untapered. To achieve a similar leading edge size, the taper rate is required to be extremely aggressive, since the maximum radius for these screws is achieved within half rotation. Figure 14 shows the variation of figure of merit for these screws, indicating a better performance when the second half is left untapered. Furthermore, the figure of merit is observed to decrease with increasing taper rate, as is seen with uniformly tapered aerial screws.

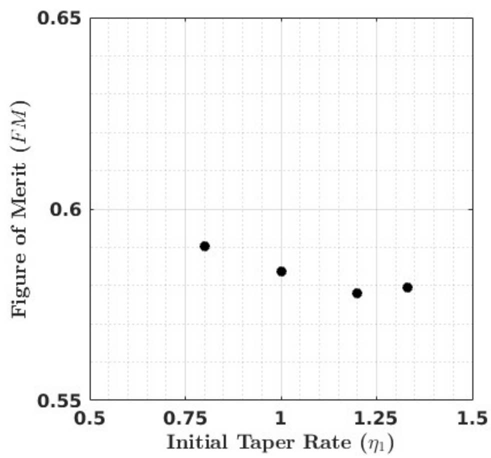

Figure 14. Variation of figure of merit of bilinearly tapered aerial screws with varying initial taper rate

Figure 15 shows the surface normal loads and their axial and torque-wise components for the best performing screw with $\eta_1 = 0.8$. It can be seen that the strength of the da Vinci vortex is maintained along the first half screw surface where the screw is tapered. The strength of the vortex lowers along the downstream in the untapered region of the screw. This is because the vortex is no longer bound to the tip of the screw as the vortical structure is no longer strengthened by the untapered blade. However, the strength of the vortex built in the first half blade region is sufficiently sustained through the next half rotation, rendering the surface active in thrust generation.

These results indicate that aggressive taper is not beneficial for the aerodynamic performance of the screw. Low to moderate taper is however required for the da Vinci vortex to be developed and confined to the tip of the screw surface.

Effect of Number of Blades (N_b)

The screws considered for this study are with a uniform taper rate $\eta = 0.5$, uniform pitch rate $\zeta = 1.3$ and radius of 1 ft. Figure 16 shows the variation of figure of merit for these screws, indicating a continuous and significant decrease in the performance with increasing number of blades. This is consistent with the conventional low solidity helicopter rotors, and is

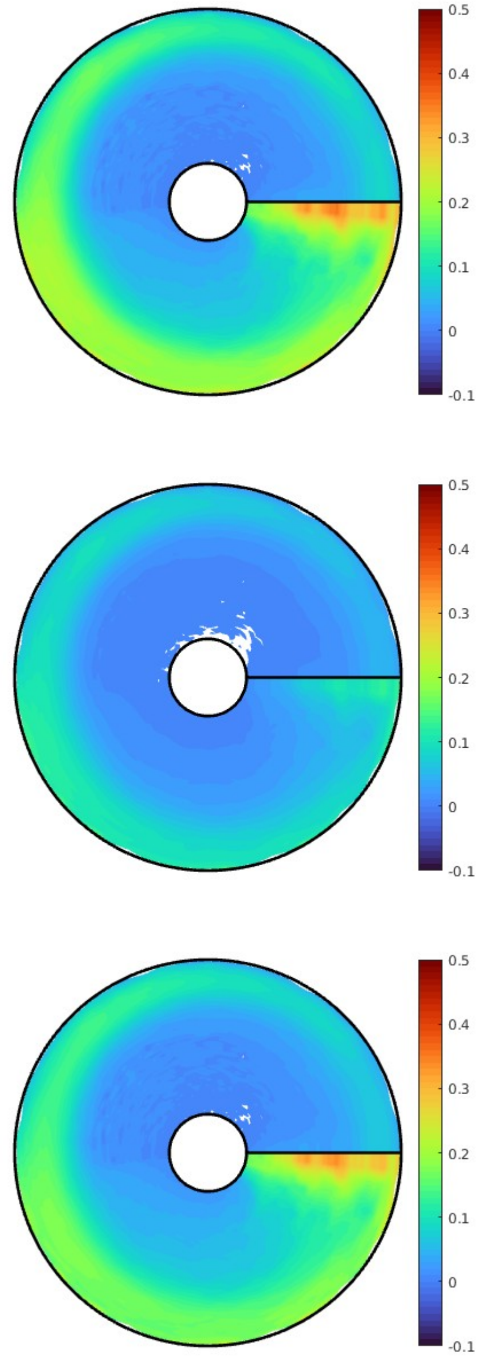

Figure 15. Surface load projections onto $r' - \theta$ plane for aerial screw with $\zeta = 1.3$ and bilinear taper with $\eta_1 = 0.8$, Top: ΔC_P, Middle: Axial component and Bottom: Torque-wise component

due to the interactional aerodynamics between multiple blades increasing the losses.

Figure 17 shows the vorticity iso-contours for these screws, indicating the reduction in da Vinci vortex strength with increasing number of blades. Furthermore, it is observed that the vortex moves inboard with increasing number of blade, due to the interactions between other helical vortical struc-

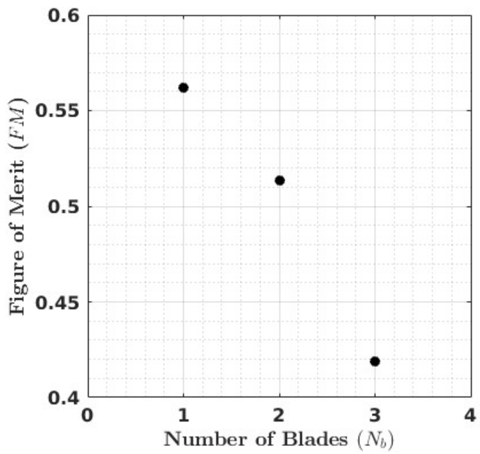

Figure 16. Variation of figure of merit with number of blades

tures.

While the performance is worsened with increasing number of blades, all these screws have the same taper and pitch characteristics. While these values correspond to a better performance for a single bladed screw, it is not necessary that the same geometric variation is suitable for multiple blades. Hence, a combination of the design variable variations such as increase in pitch with increasing umber of blades may improve the performance substantially.

CONCLUSIONS

This study presents an in-depth exploration of the aerodynamic principles governing the performance of aerial screws, inspired by Leonardo da Vinci's early concepts. By leveraging modern Computational Fluid Dynamics (CFD) tools, the research elucidates the role of key geometric design variables on the thrust generation mechanism and overall aerodynamic efficiency of the aerial screws.

The analysis reveals that the "da Vinci vortex," a shape-conforming helical vortical structure at the screw's tip, is central to the thrust production in aerial screws. This mechanism is similar to vortex lift phenomena observed in swept and delta wings, where it contributes significantly to pressure differentials across the screw surface, thereby enhancing thrust.

The influence of each design variable on the aerodynamic performance of aerial screws is studied. The key findings include:

- Influence of Screw Radius: Increasing the screw radius generally enhances the figure of merit, indicating improved aerodynamic efficiency. However, the rate of improvement diminishes with larger screw sizes, suggesting a potential trade-off between aerodynamic performance and practical design considerations.
- Effect of Pitch Rate: The pitch rate critically affects the screw's performance. A moderate increase in pitch rate enhances the figure of merit, attributed to optimized

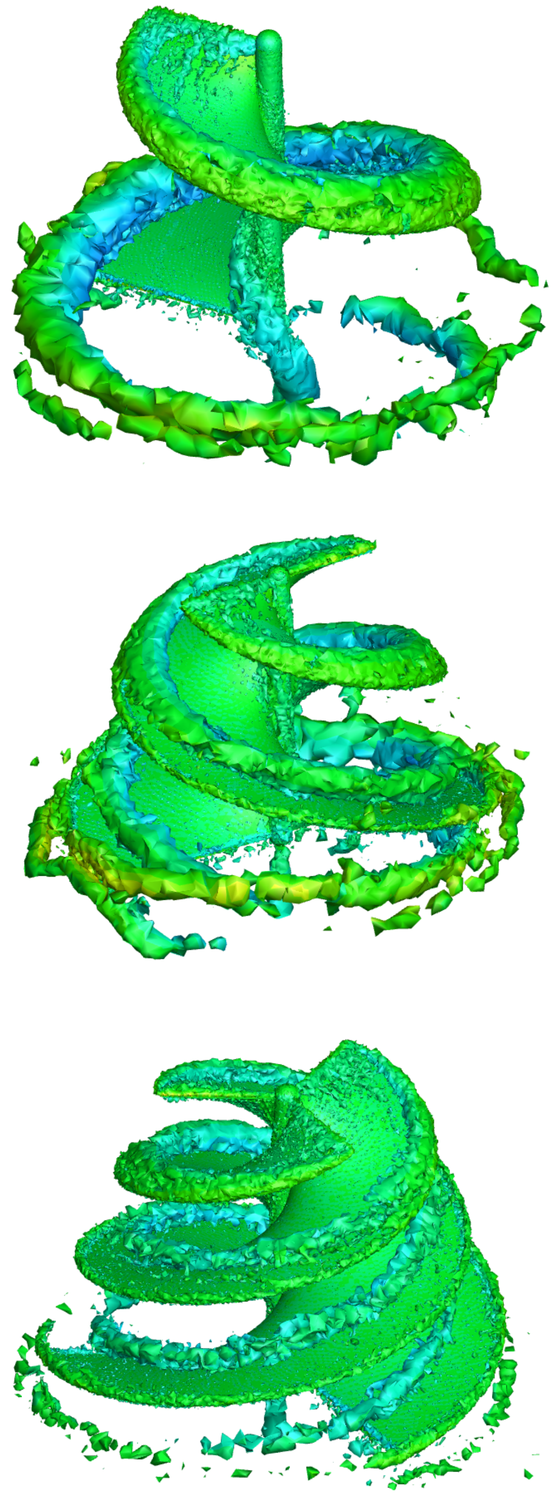

Figure 17. Vorticity contours showing the decreased strength of daVinci vortex with increasing number of blades in the screw

vortex formation and pressure distribution. However, an aggressive pitch rate leads to significant increases in torque-wise loads, which diminish overall efficiency and highlight the importance of balancing pitch to optimize performance.

- Effect of Taper Rate: The taper rate modifies the screw surface's gradient, directly impacting the contribution of normal forces to axial thrust. A well-calibrated taper rate can lead to enhanced thrust production by optimizing the axial component of pressure forces, particularly in the downstream sections of the screw.

- Effect of Blade Number: The study identifies that an increase in number of blades significantly lowers the performance of the aerial screws, when the other design variables are unaltered.

Achieving figures of merit as high as 0.55 with variations in just one design variable, and 0.59 with nonlinear design variables, this study highlights the considerable potential of these rotors for efficient design. The aerial screws, when meticulously designed, show promise as a suitable alternative for Vertical Take-Off and Landing (VTOL) applications, particularly at smaller scales, offering an innovative alternative to conventional rotor designs.

Future work could focus on further refinement of these design parameters, including the effects of dihedral angles, nonlinear tapering, and multi-bladed configurations, to fully unlock the potential of aerial screws in modern VTOL applications. Moreover, experimental validation of the CFD predictions would provide further confidence in the applicability of these findings to real-world aerial screw designs.

Author contact:
Koushik Marepally *koushikm@umd.edu*
Ron Berlin *rberlin8@terpmail.umd.edu*

ACKNOWLEDGMENTS

The authors would like to thank the University of Maryland's high performance computing resource Zaratan, which was used for the CFD simulations in this study.

REFERENCES

1. Lambermont, P., and Pirie, A., *Helicopters and Autogyros of the World*, Barnes, 1970.

2. Baden-Powell, B., "Experiments with Aerial Screw Propellers," *Aeronautical journal (London, England: 1897)*, Vol. 8, (30), 1904, pp. 28–32. DOI: 10.1017/S2398187300142380.

3. Leonardo Helicopters, "37th Annual Student Design Competition - 2019-2020 Request for Proposal (RFP) - Leonardo's Aerial Screw: 500 Years Later," .

4. Sutherland, J., Brown, R., Ebewele, E., Fisler, E., Krohmaly, K., Linkins, J., Marepally, K., Prete, A., Semenov, I., Nagaraj, V., Chopra, I., and Datta, A., "Leonardo's Aerial Screw: 500 Years Later," University of Maryland, 2020.

5. Prete, A., Nagaraj, V., and Chopra, I., "Revolutionary Flight Vehicle Based on Leonardo da Vinci Aerial Screw: A Paradigm Shift in VTOL Technology," VFS Aeromechanics for Advanced Vertical Flight Technical Meeting, San Jose, CA, Jan 25-27, 2022, 2022.

6. Prete, A. C., *Revolutionary flight vehicle based on Leonardo Da Vinci Aerial Screw: a paradigm shift in VTOL Technology*, Master's thesis, University of Maryland, College Park, 2022.

7. Polhamus, E. C., "A concept of the vortex lift of sharp-edge delta wings based on a leading-edge-suction analogy," NASA TN D-3767, 1966.

8. Jung, Y. S., Govindarajan, B., and Baeder, J., "A Hamiltonian-Strand Approach for Aerodynamic Flows Using Overset and Hybrid Meshes," VFS 72nd Annual Forum, West Palm Beach, Florida, 05 2016.